

Original scientific paper

Ključne reči:
hibridni fotonaponski sistemi;
pasivno hlađenje; upravljanje
toplotom

OPTIMIZACIJA EFIKASNOSTI FOTONAPONSKIH SISTEMA PUTEM PASIVNOG I AKTIVNOG HLAĐENJA: PROCENA DVOSTRUKOG PRISTUPA PVT

Key words:
hybrid photovoltaic systems;
passive cooling; thermal
management

OPTIMIZING PHOTOVOLTAIC EFFICIENCY THROUGH PASSIVE AND ACTIVE COOLING: A DUAL-APPROACH ASSESSMENT

Marius-Costel BALAN*

* marius-costel.balan

@academic.tuiasi.ro

Andrei BURLACU

Robert-Ștefan VIZITIU

Ștefanica-Eliza VIZITIU

Technical University "Gh. Asachi" of Iasi, Romania
ORCID 0000-0002-8285-6640

Technical University "Gh. Asachi" of Iasi, Romania
ORCID 0000-0002-3926-421X

Technical University "Gh. Asachi" of Iasi, Romania
ORCID 0000-0001-5806-4902

Technical University "Gh. Asachi" of Iasi, Romania
ORCID 0000-0003-1196-7164

Operativna efikasnost fotonaponskih modula u velikoj meri zavisi od temperature ćelija, koja ima tendenciju značajnog porasta pod kontinuiranim izlaganjem suncu, što dovodi do smanjenja električnog izlaza. Ovaj rad predstavlja sveobuhvatno eksperimentalno i numeričko istraživanje dve strategije upravljanja toplotom – pasivnog i aktivnog hlađenja – primenjenih na hibridne fotonaponsko-termalne (PVT) module.

U pasivnoj konfiguraciji, toplotne cevi su pričvršćene na zadnju stranu PV modula kako bi se višak toplote disipirao prirodnom konvekcijom. Eksperimentalni testovi i CFD simulacije pokazali su smanjenje temperature od 12–20 °C korišćenjem uskih toplotnih cevi i 14–18 °C korišćenjem širokih toplotnih cevi, što je dovelo do poboljšanja električne efikasnosti od 4,5–7,1% i 5,2–6,6%, respektivno. Šire toplotne cevi pokazale su superiorne termalne performanse zahvaljujući povećanoj kontaktnoj površini i boljoj raspodeli toplote.

Za aktivno hlađenje, istražena su tri sistema zasnovana na vodi: serpentina, header-riser i višestruka serpentina. Hlađenje je postignuto kontinuiranom cirkulacijom vode, a eksperimenti su pokazali prosečno smanjenje temperature ćelija do 31 °C. Električna efikasnost poboljšana je za 6,4–11,6%, dok je termalna efikasnost dostigla vrednosti između 62% i 83%, u zavisnosti od konfiguracije. Među svim testiranim rešenjima, sistem header-riser pokazao se kao najefikasniji, postigavši ukupnu efikasnost veću od 90% u optimalnim uslovima. Analiza raspodele temperature putem infracrvene termografije potvrdila je ravnomernije hlađenje u aktivnim sistemima, naročito u konfiguraciji header-riser.

Međutim, pasivno hlađenje ostaje privlačno za aplikacije sa niskim zahtevima za održavanje, zahvaljujući svojoj jednostavnosti i odsustvu potrebe za dodatnom energijom. Nalazi potvrđuju da oba metoda – pasivno i aktivno hlađenje – značajno poboljšavaju performanse PVT modula, pri čemu svaki nudi prednosti u zavisnosti od ograničenja primene, kao što su složenost sistema, energetska autonomija i klimatski uslovi.

The operational efficiency of photovoltaic modules is highly dependent on cell temperature, which tends to rise significantly under continuous solar exposure, resulting in reduced electrical output. This paper presents a comprehensive experimental and numerical investigation of two thermal management strategies, passive and active cooling, applied to hybrid photovoltaic-thermal modules. In the passive configuration, heat pipes were attached to the rear side of PV modules to dissipate excess heat through natural convection. Experimental tests and CFD simulations demonstrated a temperature reduction of 12–20 °C using narrow heat pipes and 14–18 °C using wide heat pipes, leading to electrical efficiency improvements of 4.5–7.1% and 5.2–6.6%, respectively. The wider heat pipes showed superior thermal performance due to their increased contact area and improved heat spread. For active cooling, three water-based systems were investigated: serpentine, header-riser, and multiple-serpentine heat exchangers. Cooling was achieved through continuous water circulation, and experiments revealed average cell temperature reductions of up to 31 °C. Electrical efficiency improved by 6.4–11.6%, while thermal efficiency reached values between 62% and 83% depending on the configuration. Among all tested solutions, the header-riser system proved most effective, achieving a total efficiency exceeding 90% in optimal conditions. Temperature distribution analysis via infrared thermography confirmed more uniform cooling in the active systems, especially in the header-riser configuration. However, passive cooling remains attractive for low-maintenance applications due to its simplicity and lack of power requirements. The findings confirm that both passive and active cooling methods significantly enhance PVT module performance, each offering advantages depending on application constraints such as system complexity, energy autonomy, and climatic conditions.

1. Introduction

Photovoltaic energy conversion is widely regarded as one of the most promising renewable technologies for electricity generation, offering a clean, sustainable and locally available source of power. PV systems are characterised by their long operational lifetime, absence of direct CO₂ emissions and minimal transmission losses due to on-site production [1], [2]. However, the thermal behaviour of photovoltaic modules remains a critical limitation. Even a modest temperature increase of 1 °C can reduce electrical output by approximately 0.65–0.85 % [3], and during summer operation PV cell temperatures may rise to 40–70 °C, leading to efficiency losses in the range of 7.5–22.5 % [4]. Over the years, numerous passive cooling strategies have been proposed, some experimentally validated, others remaining largely conceptual, to mitigate this thermal penalty. These developments provide the foundation for exploring more advanced or hybrid cooling approaches introduced in recent studies.

Passive cooling solutions for photovoltaic modules can generally be classified into two categories: direct and indirect systems. Direct cooling approaches rely on a heat sink that is physically attached to the back surface of the PV panel, enabling immediate heat dissipation. In contrast, indirect cooling systems employ an intermediate heat-transfer mechanism, such as heat pipes, to transport thermal energy away from the module toward a remote heat sink or the surrounding air [5]. A relevant example of passive cooling implementation is the experimental study conducted by [6], which investigated the performance of fin-based heat sinks combined with a planar reflector under the climatic conditions of the National University of Malaysia. Among the tested configurations, lapping fins exhibited the best performance, reducing module temperature to 24.6 °C and yielding an electrical efficiency of 10.68% and a power output of 37.1 W under irradiance of 1000 W/m² and 33 °C ambient temperature.

Further contributions to passive PV cooling optimization include the work of S.N. Razali et al. (2023), who examined multidirectional tapered fin heat sinks manufactured from aluminium alloy. Their findings indicated a temperature reduction of approximately 12 °C and an electrical efficiency increase of 1.53% when compared with an uncooled reference panel under identical operating conditions. These results highlight tapered fin heat sinks as a promising and robust solution for enhancing PV performance in thermally demanding tropical climates [7].

To further connect these developments with the core topic of heat-pipe-based passive cooling, it is important to note that several recent studies have already demonstrated the potential of such systems. In 2024, Yahya Sheikh et al. designed and evaluated a hybrid cooling configuration integrating heat pipes and a bio-based phase change material (PCM). The choice of using heat pipes, rather than directly attaching the PCM to the PV surface, was motivated by the low thermal conductivity of most PCMs. By coupling the condenser section of the heat pipes with an aluminium flat plate, the system benefited from enhanced contact area and improved convective heat transfer to the surrounding air. Across four tested configurations, the most effective case achieved a temperature reduction of 37 °C under a radiative heat flux of 1000 W/m² and an electrical efficiency increase of up to 17.3%, outperforming other PCM or heat-pipe-only cooling strategies presented in the literature [5].

Passive cooling methods for photovoltaic panels include several approaches, among which phase change material (PCM)-based systems represent a distinct category. Unlike heat-pipe cooling strategies, PCM-based concepts rely on the solid–liquid phase transition to absorb and store thermal energy during operation [8]. A typical PV/PCM integrated configuration consists of a photovoltaic module coupled with a PCM container fabricated from a high–thermal-conductivity metal, ensuring effective heat transfer between the panel and the phase change medium [9]. Both numerical and experimental studies have been extensively conducted to evaluate the thermal performance of PV systems employing PCM cooling.

With regard to pure PCM configurations, several simulation studies have analysed the governing parameters influencing PV cooling performance. Kant et al. [10] investigated the effects of natural convection within the molten PCM, ambient wind speed, and PV panel tilt angle on the thermal regulation of a PV/PCM system. Using RT35 as the working PCM, their results showed that when both convective and conductive heat transfer mechanisms were considered, the PV panel temperature could be reduced by up to 6.0 °C.

For experimental investigations, [11] analysed the cooling performance of photovoltaic panels equipped with various multi-layer PCM configurations. Their results showed that, compared with a reference PV panel using a single PCM layer of OM42, the configurations employing OM37/OM37/OM42 and OM37/OM42/OM42 achieved temperature reductions of 3.0 °C and 1.9 °C, respectively.

Traditional PCM-based cooling strategies for PV systems typically involve attaching a solid container filled with phase change material to the rear surface of the module to regulate its operating temperature. [12] investigated an alternative configuration in which multiple smaller PCM containers were used instead of a single large unit. Their experimental results demonstrated that, relative to an uncooled reference module, the power output increased by 2.5% when using one large PCM container and by 10.7% when using several smaller containers. A comparable approach and similar findings were reported by [13].

The cooling effectiveness of phase change materials is often constrained by their inherently low thermal conductivity [14]. One widely explored approach to overcoming this limitation involves enhancing the PCM with high-thermal-conductivity additives, such as nanoparticles [15], or by coupling the PCM with auxiliary working fluids through hybrid thermal management strategies.

For example, [16] conducted an experimental investigation on paraffin wax enhanced with Al_2O_3 nanoparticles and multi-wall carbon nanotubes. Their results showed that nanoparticle doping significantly improved the thermal properties of the base PCM. Similarly, [17] experimentally developed a paraffin-based composite PCM containing TiO_2/Ag hybrid nanoparticles for photovoltaic cooling applications.

An essential characteristic of photovoltaic cells is their wavelength-dependent spectral response [18]. As a result, only a specific portion of the solar spectrum can be converted into electrical energy, while the remaining non-utilized radiation is absorbed as heat, elevating the module temperature and decreasing photoelectric efficiency [19]. Although conventional PV/T systems partially address this issue, the outlet temperature of the working fluid remains constrained by the temperature of the PV panel itself [20]. By contrast, PV/T systems employing spectral beam splitting can both reduce PV cell temperature and remove the thermal limitations imposed on the working fluid, thereby enhancing overall system performance.

Among the studies exploring solid beam splitters, [21] experimentally investigated a PV/T configuration incorporating a $\text{SiO}_2/\text{TiO}_2$ thin-film beam splitter. Their results indicated that the spectral filtering provided by this film reduced PV module temperature by approximately $3.0\text{ }^\circ\text{C}$.

Kandilli [22] conducted both experimental and thermodynamic analyses on a beam-splitting PV/T system employing dish concentrators in combination with hot-mirror beam splitters. The study reported an overall energy efficiency of 7.3% for the system, along with a power generation cost of 6.37 USD/W.

Wang et al. [23] proposed a solar beam-splitting PV/T system that integrates a compact linear Fresnel reflector (CLFR) with a $\text{Na}_3\text{AlF}_6/\text{Nb}_2\text{O}_3/\text{Ge}$ thin-film beam splitter. Their performance assessment showed that the system achieved an overall efficiency of 26.7%, exceeding the efficiency of a conventional concentrated photovoltaic (CPV) system, which was reported at 23.8%.

Another efficient way for cooling is heat pipe cooling. Heat pipe is an effective passive heat transfer element which utilizes phase change in a medium inside a fully enclosed vacuum pipe for heat transfer. It mainly consists of three parts, namely, evaporation, insulation, and condensation sections [24]. The heat transfer inside a heat pipe primarily depends on the gas-liquid phase change in the working fluid and does not require a large temperature difference between the heat source and the heat sink. It can have high temperature uniformity, high thermal conductivity, and variable heat flux without additional energy consumption [25]. Additionally, heat pipes also have advantages of low cost, high reliability, long service life, and diverse structure and can be freely designed according to the heat dissipation requirements and structural characteristics of different PV systems. Concentrated solar photovoltaic (CPV) systems with heat pipe cooling can not only obtain effective cooling effects for PV panels but also collect some heat for thermal utilization. When heat pipes for PV systems are designed, water, ethanol, ammonia, toluene, pentane, and other materials can be selected as the working fluid.

Hu et al. [26] conducted some experiments on solar PV/T systems using heat pipes without a wick and with a wire mesh, respectively. Figures 18 and 19 present the diagram of the studied PV/T system and two kinds of heat pipes. The effect of the tilt angle on the thermal performance of the PV/T system was evaluated. The results demonstrated that the thermal performance of the heat pipe

without a wick was sensible to the tilt angle, while that of the heat pipe with a wire mesh was not sensible to the tilt angle.

Natural air circulation is one of the simplest and most widely used passive cooling techniques for photovoltaic modules. In this approach, heat is removed from the PV panel through buoyancy-driven airflow either along the front surface or, more typically, the rear side of the module. The cooling effect can be further enhanced by integrating heat sinks on the back of the PV panel, which promote additional convective heat transfer [19]. These heat sink, commonly metallic fins, absorb heat from the PV surface and dissipate it into the surrounding environment [27]. Optimizing fin geometry, increasing surface area, or modifying fin layout are well-established strategies for improving cooling effectiveness [28].

In their study, [29] experimentally investigated the influence of fin parameters on PV temperature and electrical output under natural convection. Their findings showed that fins with dimensions of 7.0 cm × 20.0 cm provided the best performance, yielding an increase of 9.4 W in electrical power compared with an uncooled panel. A related study evaluated the use of porous fins for air-based passive cooling. The experimental results demonstrated a power increase of 7.26 W when porous fins were applied [30].

Kong et al. [31] carried out an experimental performance assessment of a roof-mounted building-attached photovoltaic (BAPV) system incorporating a double-channel air-flow cooling configuration. In their design, the PV installation featured two parallel ventilation channels intended to enhance natural air circulation beneath the module. Experimental results showed that, compared with a conventional BAPV system, the double-channel configuration achieved a temperature reduction of 6.2 °C and delivered a 4.5% increase in average electrical output power.

In this context, the present work examines both passive and active cooling strategies applied to monocrystalline PV modules, with particular emphasis on their integration into hybrid PVT systems for building applications. The thermal–electrical performance of several in-house developed prototypes is experimentally evaluated and compared against two commercially available PVT collectors tested under identical boundary conditions. By combining comprehensive experimental measurements with validated numerical simulations, the study delivers a consistent set of performance indicators related to PV temperature reduction, electrical efficiency enhancement and recoverable thermal energy. The findings provide insights into the design considerations required for next-generation PVT absorbers aimed at supporting nZEB and zero-carbon building concepts.

2. Materials and methods

2.1. Solar simulator and baseline photovoltaic characterization

The experimental campaign was performed using a laboratory-grade indoor solar simulator engineered to provide controlled and repeatable irradiance conditions for PVT testing. Illumination was supplied by a 300 W OSRAM Ultra Vitalux high-pressure mercury-vapor lamp, selected for its stable spectral output. Uniformity and irradiance levels were verified prior to testing using an RS PRO IM-750 solarimeter.

The simulator consists of a 1652 × 1000 mm metallic enclosure mounted on a mobile steel frame and equipped with twelve lamp apertures arranged in three vertical rows. Irradiance mapping was conducted both during initial calibration and after full assembly over the 1600 × 960 mm active area corresponding to the tested PV panel. Seventy-seven measurement points (160 mm spacing) were used to assess field uniformity for simulator-to-module distances between 10 and 100 cm, with contour maps generated in TopoLT to determine operational testing conditions.

The reference photovoltaic module was a monocrystalline silicon panel comprising sixty 156×156 mm cells (active area ≈ 1.46 m²). Baseline measurements were obtained at irradiance levels of 400, 353, and 302 W·m⁻², corresponding to simulator distances of 20, 30, and 40 cm. Rear-surface temperatures were monitored using twenty-four K-type thermocouples arranged in a 6×4 grid; reduced-sensor measurements employed four central thermocouples and an experimentally derived +8.5 °C correction factor. These data, supported by CFD simulations, established the thermal and electrical reference behaviour of the uncooled module. Under baseline conditions, electrical efficiency ranged from 16.95% to 17.62%, showing the expected inverse dependence on operating temperature.

2.2. PVT cooling configurations

To ensure a consistent comparison between cooling strategies, all active and passive configurations were mounted on the same monocrystalline PV module and tested under identical irradiance and boundary conditions. Each system was integrated onto a custom aluminium thermal plate designed to provide uniform rear-side contact and minimise interface resistance.

2.2.1. Active cooling modules

Three active photovoltaic–thermal (PVT) configurations were developed using the Jinko Eagle PERC JKM315M-60-V module (60 cells, 19.24% nominal efficiency, $-0.37\%/^{\circ}\text{C}$ temperature coefficient). All systems incorporated a 1.5 mm aluminium absorber plate bonded to the PV backsheet, onto which copper tube networks were mounted to allow closed-loop water circulation. Tube–plate contact was enhanced using thermal paste, and all systems shared identical hydraulic components (reservoir, variable-speed pump, flow control, inlet/outlet thermocouples).

2.2.1.1. Register-type configuration

This design used vertically oriented 10 mm copper tubes spaced at 20 mm, supplied by 15 mm lower and upper manifolds. It represents the simplest configuration, offering uniform hydraulic distribution with minimal pressure drop.

2.2.2.1. Single serpentine configuration

A continuous 10 mm copper serpentine (30 mm bending radius) covered the entire absorber surface. The extended contact length improved thermal uniformity but increased hydraulic resistance relative to the register-type system.

2.2.3.1. Multi-serpentine configuration

Ten parallel serpentine branches (10 mm tubes) were connected to 15 mm inlet and outlet manifolds. The parallel arrangement significantly reduced pressure losses and improved lateral temperature uniformity, particularly at higher flow rates. All active systems were mounted on identical support frames, aligned with the solar simulator, and tested under the same irradiance, ambient and hydraulic conditions, enabling direct comparison with passive prototypes and two commercial PVT collectors. The designs are presented in figure 1.

2.2.5. Passive cooling modules

Two passive systems based on flattened heat pipes (HPs) were developed to enable non-powered thermal regulation. Heat pipes were selected for their high effective thermal conductivity and capillary-driven phase-change operation. A $1620 \times 960 \times 10$ mm aluminium thermal plate was fabricated for both designs, including a junction-box cut-out. Two HP geometries were evaluated: Narrow

copper HPs (300 mm length, 10.65×4 mm flattened profile, water as working fluid; capacity 17–26 W) and Wide aluminium HPs ($250 \times 50 \times 2.5$ mm, acetone working fluid; capacity 75–300 W).

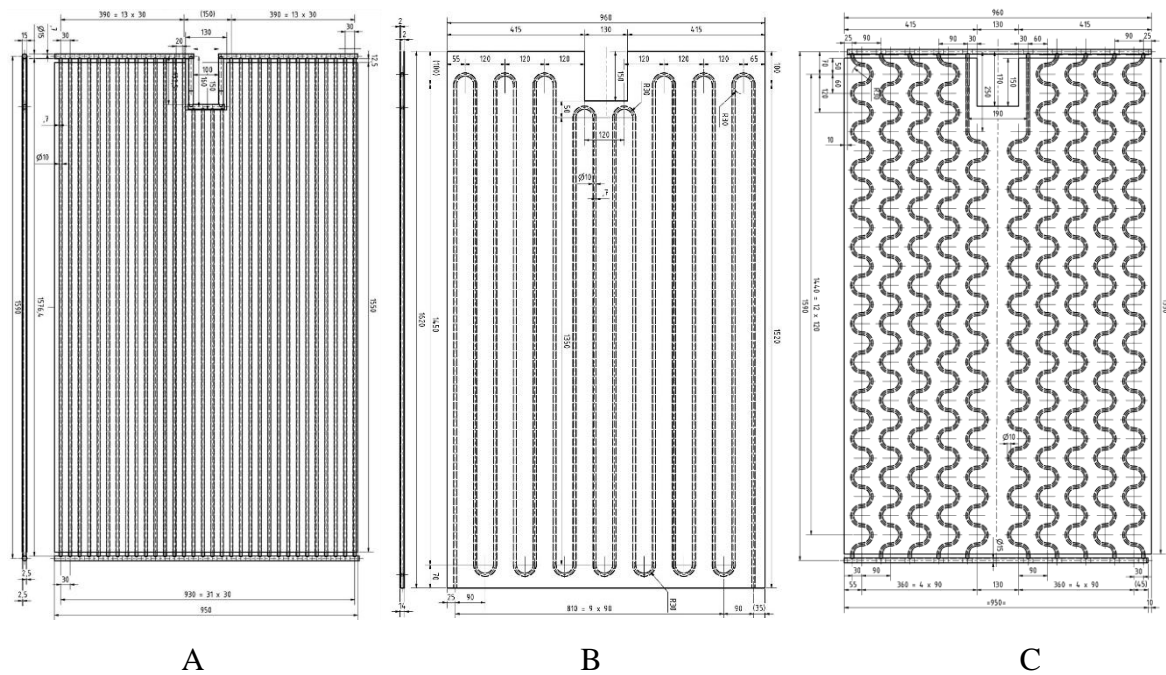


Figure 1. Constructive details of the cooling system configurations: A – Register-type configuration, B – Single-serpentine configuration, C – Multi-serpentine configuration

2.2.5.1. Narrow heat-pipe configuration

Sixty-three copper HPs were arranged in a 7×9 array. Pipes were inserted into dedicated evaporator and penetration cavities and angled at 45° to promote condensate return. Spacing was optimised to maximise coverage of the PV active area.



PV panel with wide HP



PV panel with narrow HP

Figure 2. Narrow (copper) and wide (aluminium) flattened heat pipes employed in the passive PVT cooling modules.

2.2.6.1. Wide heat-pipe configuration

Forty aluminium HPs were mounted in a 5×8 array using larger recesses to increase the evaporator footprint and enhance heat extraction relative to the narrow HP system.

C. Assembly and integration

Both passive modules were assembled following a controlled procedure involving CNC machining, surface preparation, application of thermal paste, insertion and alignment of HPs, and bonding of the plate to the PV rear surface. Temperature sensors were positioned to allow detailed mapping of surface temperature fields. Passive systems operated exclusively through evaporation–condensation cycles and were tested under the same irradiance and ambient conditions as the active modules and commercial PVT collectors.

2.3. Instrumentation and experimental setup

A dedicated instrumentation system was implemented to measure the thermal and electrical performance of all cooling configurations. Temperature data were recorded using a Lutron BTM-4208SD multi-channel logger connected to K-type thermocouples. Surface temperatures on the PV/PVT rear side were measured with exposed-junction probes, while immersion probes were used for inlet and outlet fluid temperatures in active systems. All sensors were calibrated before testing, and temperature stability during measurements was maintained within ± 1.5 °C (ambient) and ± 0.2 °C (inlet).

Hydraulic measurements were performed using a solar pumping group equipped with a Grundfos UPM3 15-105 circulator. Flow rate regulation and verification were provided by a TacoSetter Inline 130 flow meter, while thermal power and fluid temperatures were monitored with an ACTARIS CF55 heat meter. A 12-L expansion vessel ensured loop pressure stability at operating temperatures up to 99 °C.

The electrical subsystem consisted of an EPEver XTRA2210N MPPT controller connected to a 200 Ah VRLA gel battery and an IPower pure-sine inverter for AC loads. Electrical parameters were logged via an EPEver eLOG-01 RS485 module at ten-minute intervals, enabling continuous tracking of power output and operational states.

All experiments were conducted under controlled laboratory conditions using the same solar simulator, identical mounting frames, and strict boundary-condition stability (ambient ± 1.5 °C, inlet ± 0.2 °C, flow variation $< \pm 5\%$). A complete thermal–hydraulic–electrical schematic of the experimental setup, including the PV/PVT module, circulation loop, instrumentation layout and absorber/heat-pipe assemblies, is presented in Figure 3.

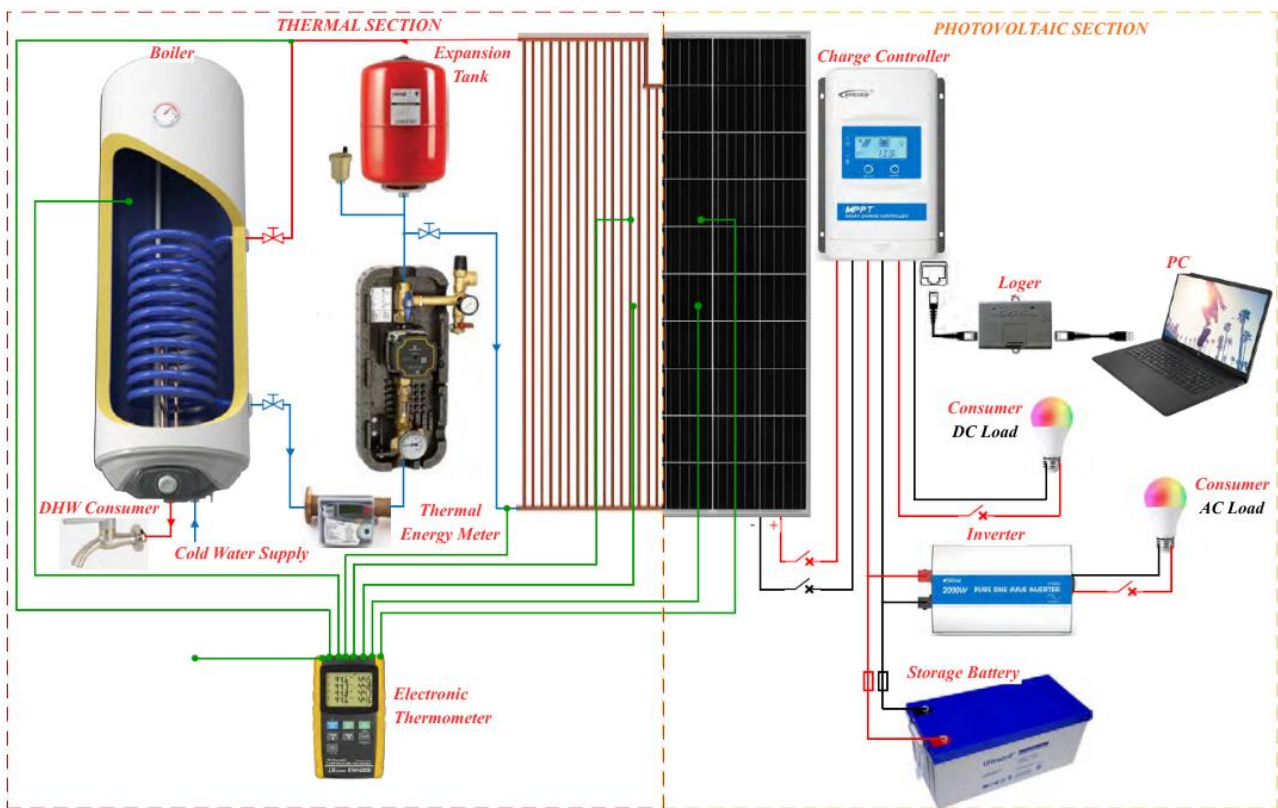


Figure 3. General schematic of the experimental stand

3. Experimental results and discussion

3.1. Baseline PV behaviour under artificial solar irradiance

Baseline tests were conducted to establish the thermal and electrical behaviour of the uncooled monocrystalline PV module under controlled irradiance conditions. The module incorporates sixty 156×156 mm cells (active area ≈ 1.46 m²), and its rear-surface temperature field was initially characterised using 24 contact thermocouples arranged in a 6×4 grid. These measurements consistently indicated that the central region of the module exhibited the highest temperatures. Accordingly, subsequent experiments employed four centrally located sensors together with an experimentally derived correction factor of $+8.5$ °C to reconstruct the average module temperature.

The influence of irradiance was evaluated by adjusting the simulator–module distance to 20, 30 and 40 cm, corresponding to the most uniform illumination levels identified during calibration. Distances below 20 cm generated significant non-uniformity and hot spots, while distances above 50 cm introduced ambient-light interference, increasing measurement uncertainty to around $\pm 3\%$.

Under steady-state operation, the PV module experienced a continuous temperature rise during the one-hour exposure period, stabilising at 67.69 °C, 63.03 °C and 59.51 °C for simulator distances of 20, 30 and 40 cm, respectively. Since all three levels yielded similar thermal trends, Figure 6 illustrates the temperature evolution for the 40 cm case, expressed as the time-averaged value from all 24 thermocouples. Numerical simulations reproduced these measurements with deviations below 0.5 °C, demonstrating the accuracy of the thermal model later applied to the PVT configurations.

Extended baseline testing also showed that localised temperatures could approach 80 °C, close to the manufacturer's recommended limit of 85 °C. Even under controlled indoor conditions, the module therefore operated under considerable thermal stress, contributing to reduced electrical efficiency and accelerated ageing. These results form the reference against which all passive and active cooling strategies are evaluated in the subsequent sections.

3.2. *Passive cooling with flattened heat pipes*

Two passive cooling configurations based on flattened heat pipes were evaluated to assess their ability to reduce PV operating temperature without external power input. Both systems were mounted on identical aluminium transfer plates covering the full rear active area of the module. The first configuration employed 63 narrow copper heat pipes arranged in a 7×9 matrix, whereas the second used 40 wide aluminium heat pipes arranged in a 5×8 matrix. All pipes were bent at 45° to enhance condensate return and ensure proper alignment between the evaporator section and the PV backsheet.

The copper heat pipes, charged with distilled water, offered heat transport capacities of 17–26 W depending on evaporator–condenser spacing. The wide aluminium heat pipes, operating with acetone, provided substantially higher transport capacity (up to 300 W) due to their larger contact footprint and rectangular geometry. These intrinsic structural and working-fluid differences resulted in distinct thermal performance.

Both assemblies were bonded to the PV rear surface using high-conductivity thermal paste and tested under the same irradiance levels as the baseline module. Temperature evolution was monitored using the reduced sensor array and verified through numerical simulations.

The narrow heat-pipe system reduced the average PV temperature by 12–20 °C across all irradiance levels, while the wide heat-pipe system achieved reductions of 14–18 °C. Thermal maps indicated that the wide heat pipes produced superior lateral temperature uniformity, consistent with their higher effective conductivity and larger evaporator contact area.

Electrical performance improvements mirrored these trends. The narrow copper HP configuration increased electrical efficiency by 4.5–7.1%, whereas the wide aluminium HP design yielded gains of 5.2–6.6%. Since both configurations operate exclusively through passive evaporation–condensation cycles, they impose no hydraulic or electrical consumption and are well suited for standalone or low-maintenance PVT applications.

Overall, both passive modules demonstrated substantial thermal mitigation under controlled laboratory conditions. Given that outdoor operation would introduce natural convective cooling of the condenser section, even higher performance may be expected in real environments. Among the two concepts, the wide heat-pipe configuration proved the most effective, offering improved temperature uniformity, greater heat-transport capability and higher electrical-efficiency enhancement.

3.3. *Active water-cooled configurations*

Three active water-cooled PVT configurations were evaluated to determine the influence of cooling geometry on heat extraction, temperature uniformity and hybrid electrical–thermal performance. All systems were mounted on the same monocrystalline PV module and tested under three irradiance levels (simulator distances of 20, 30 and 40 cm). For each irradiance level, volumetric flow rates of 0.5, 1.5 and 2.5 L/min were applied, enabling a systematic multi-scenario comparison. CFD simulations closely reproduced the measured temperature fields, confirming the robustness of the experimental results.

The single serpentine configuration demonstrated strong cooling effectiveness but exhibited pronounced longitudinal temperature gradients. It reduced PV temperature by 24–31 °C across all irradiance levels, leading to electrical-efficiency gains of 7.4–11.5%. At 2.5 L/min, outlet water reached 36–39.8 °C after 3 hours, corresponding to thermal efficiencies of 62–80%. However, the large inlet–outlet temperature difference indicated non-uniform heat extraction along the flow path.

The register configuration, consisting of parallel vertical channels supplied by lower and upper manifolds, delivered the most balanced thermal behaviour. Temperature reductions ranged from 25.5 to 31.4 °C, comparable to the serpentine but with substantially improved spatial uniformity. Electrical

efficiency increased by 6.8–11.6%, and thermal efficiency reached 62.5–82.7% depending on irradiance and flow rate. Owing to effective flow distribution, this configuration consistently achieved the highest combined PVT performance, with several scenarios exceeding 90% total efficiency and outperforming the commercial PVT benchmarks tested.

The multiple-serpentine configuration, composed of ten parallel meanders connected to common distributor–collector manifolds, showed intermediate behaviour. Temperature reductions of 17.4–21.3 °C were notably lower than those observed for the single-serpentine or register systems, reflecting limited flow penetration and increased hydraulic resistance. Electrical-efficiency gains ranged from 6.4% to 7.9%, while thermal efficiency varied between 39% and 56.8%. Although this geometry provided more uniform cooling than the single serpentine, its overall effectiveness was constrained under high-irradiance conditions.

Across all active configurations, both experiments and simulations confirm that water cooling substantially improves PV performance by maintaining lower cell temperatures and enabling significant thermal recovery. Among the tested designs, the register-type absorber exhibited the most favourable balance between thermal spreading, electrical enhancement, hydraulic performance and overall hybrid efficiency, underscoring the importance of coolant distribution geometry in PVT system design.

3.4. Synthesis of results and PVT design implications

To provide an integrated perspective on the cooling strategies analysed in this study, the experimental and numerical results were synthesised using three global indicators: PV temperature reduction, electrical-efficiency enhancement and thermal energy recovery. These metrics enabled a coherent comparison between the passive heat-pipe modules and the active water-cooled absorbers.

The passive configurations based on flattened heat pipes demonstrated consistent temperature mitigation, lowering the PV operating temperature by 12–20 °C for the narrow copper pipes and by 14–18 °C for the wide aluminium pipes. These thermal reductions resulted in electrical-efficiency gains of 4.5–7.1% and 5.2–6.6%, respectively. While passive systems do not supply thermal energy for water heating, they provide reliable cooling without parasitic power consumption and with minimal maintenance requirements. The wide heat-pipe configuration produced the most uniform temperature distribution, owing to its larger evaporator footprint and higher effective thermal conductivity, which reduced peak gradients and enhanced thermal spreading.

Among the active systems, the single-serpentine absorber offered the largest absolute temperature reduction, reaching up to 31 °C, and generated the highest electrical-efficiency improvements of the three designs. However, the pronounced inlet–outlet thermal gradient indicated non-uniform local cooling, particularly under low-flow conditions. The multiple-serpentine configuration improved lateral temperature distribution but generally operated at higher average temperatures unless supplied with larger volumetric flow rates, reflecting increased hydraulic resistance and uneven flow distribution across the branches.

The register-type absorber consistently provided the most favourable balance between cooling intensity, spatial uniformity and thermal recovery. Its parallel-channel arrangement enabled homogeneous coolant distribution with minimal hydraulic losses, producing temperature reductions of 25.5–31.4 °C and electrical-efficiency enhancements of 6.8–11.6%. Thermal efficiencies reached up to 82.7%, confirming its strong potential for hybrid PVT applications requiring simultaneous electrical and thermal output. A comprehensive comparison of the thermal behaviour of all cooling configurations is presented in Figure 4, which illustrates the time-resolved PV temperature evolution under identical irradiance conditions..

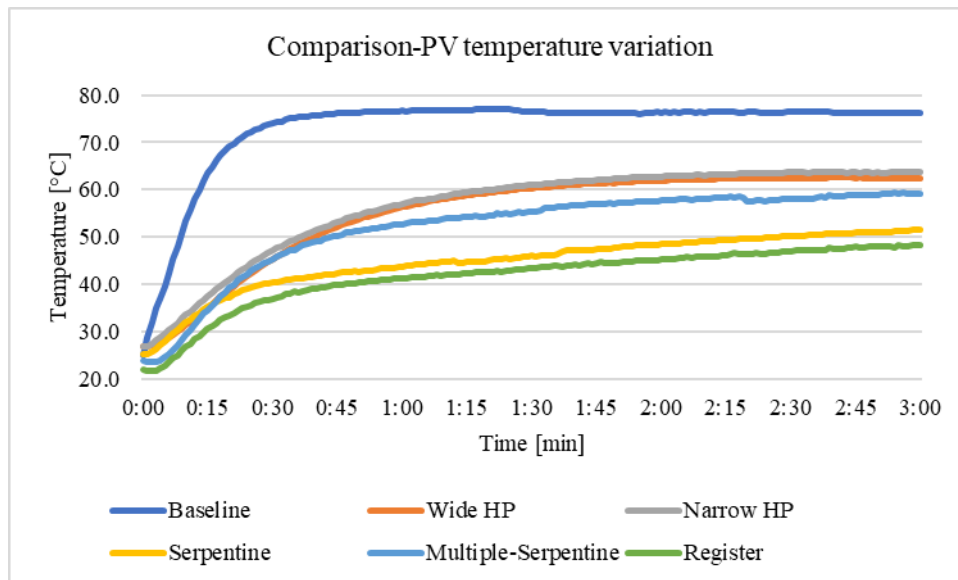


Figure 4. Comparison of PV rear-surface temperature evolution for all cooling configurations over a 3-hour test period

Overall, the comparative analysis highlights the critical role of coolant distribution geometry in determining global PVT performance. Uniform flow paths, low hydraulic resistance and effective thermal contact at the absorber–PV interface were found to be decisive factors in achieving stable and efficient heat extraction. Passive heat-pipe modules represent a viable solution for scenarios prioritising low cost and maintenance-free operation, while actively cooled absorbers—particularly the register-type design—offer superior electrical and thermal performance when water heating is desired.

4. Conclusions

This study experimentally evaluated the thermal and electrical performance of several passive and active cooling strategies for monocrystalline PV modules under controlled solar simulator conditions. The results confirm that PV operating temperature remains the dominant factor governing electrical efficiency, with the uncooled module reaching steady-state values above 60–70 °C, close to the manufacturer’s upper operating limit. All cooling approaches investigated—passive and active—provided significant thermal mitigation, thereby improving electrical output and operational stability.

Passive cooling using flattened heat pipes demonstrated reliable temperature reduction without external energy input. The narrow copper pipes achieved temperature decreases of 12–20 °C, while the wide aluminium pipes yielded reductions of 14–18 °C and superior spatial uniformity due to their larger evaporator footprint. These effects translated into electrical-efficiency gains of up to 7%, confirming the suitability of heat-pipe systems for low-maintenance PV installations where simplicity and reliability are prioritised.

Active water-cooled absorbers delivered substantially higher cooling performance. The single-serpentine configuration achieved the largest absolute temperature drop, reaching up to 31 °C, but exhibited strong thermal gradients along the flow direction. The multiple-serpentine design improved lateral heat spreading but remained limited by hydraulic resistance at lower flow rates. The register-type absorber consistently provided the most balanced behaviour, combining temperature reductions above 25 °C with excellent spatial uniformity, electrical-efficiency gains up to 11.6%, and thermal

efficiencies exceeding 80%. These findings highlight the decisive influence of coolant distribution geometry on hybrid system performance.

Overall, the study demonstrates that while passive heat-pipe systems offer robust and maintenance-free temperature control, optimised active PVT absorbers, particularly those employing parallel hydraulic layouts, can achieve substantially higher hybrid performance. The results underline the importance of tailored absorber geometries, proper thermal contact at the PV–absorber interface, and uniform coolant distribution in designing next-generation PVT technologies for building integration and nZEB applications. Future work will extend these findings through outdoor validation and long-term performance assessment under real climatic conditions.

5. References

- [1] **S. V. Hudişteanu, F. E. Ţurcanu, N. C. Cherecheş, C. G. Popovici, M. Verdeş, and I. Huditeanu**, Enhancement of PV Panel Power Production by Passive Cooling Using Heat Sinks with Perforated Fins, *Appl. Sci.*, vol. 11, no. 23, p. 11323, Jan. 2021, doi: 10.3390/app112311323.
- [2] **W. S. Ebhota and P. Y. Tabakov**, Influence of photovoltaic cell technologies and elevated temperature on photovoltaic system performance, *Ain Shams Eng. J.*, vol. 14, no. 7, p. 101984, July 2023, doi: 10.1016/j.asej.2022.101984.
- [3] **A. R. Abdulmunem, P. Mohd Samin, H. Abdul Rahman, H. A. Hussien, I. Izmi Mazali, and H. Ghazali**, Numerical and experimental analysis of the tilt angle's effects on the characteristics of the melting process of PCM-based as PV cell's backside heat sink, *Renew. Energy*, vol. 173, pp. 520–530, Aug. 2021, doi: 10.1016/j.renene.2021.04.014.
- [4] **P. Huang, G. Wei, L. Cui, C. Xu, and X. Du**, Numerical investigation of a dual-PCM heat sink using low melting point alloy and paraffin, *Appl. Therm. Eng.*, vol. 189, p. 116702, May 2021, doi: 10.1016/j.applthermaleng.2021.116702.
- [5] **Y. Sheikh, M. Jasim, M. O. Hamdan, B. A. Abu-Nabah, and F. Gerner**, Design and performance assessment of a solar photovoltaic panel integrated with heat pipes and bio-based phase change material: A hybrid passive cooling strategy, *J. Energy Storage*, vol. 100, p. 113706, Oct. 2024, doi: 10.1016/j.est.2024.113706.
- [6] **A. M. Elbreki, A. F. Muftah, K. Sopian, H. Jarimi, A. Fazlizan, and A. Ibrahim**, Experimental and economic analysis of passive cooling PV module using fins and planar reflector, *Case Stud. Therm. Eng.*, vol. 23, p. 100801, Feb. 2021, doi: 10.1016/j.csite.2020.100801.
- [7] **S. N. Razali et al.**, Performance enhancement of photovoltaic modules with passive cooling multidirectional tapered fin heat sinks (MTFHS), *Case Stud. Therm. Eng.*, vol. 50, p. 103400, Oct. 2023, doi: 10.1016/j.csite.2023.103400.
- [8] **F. Hachem, B. Abdulhay, M. Ramadan, H. El Hage, M. G. El Rab, and M. Khaled**, Improving the performance of photovoltaic cells using pure and combined phase change materials – Experiments and transient energy balance, *Renew. Energy*, vol. 107, no. C, pp. 567–575, 2017.
- [9] **M. S. Hossain, A. K. Pandey, J. Selvaraj, N. A. Rahim, M. M. Islam, and V. V. Tyagi**, Two side serpentine flow based photovoltaic-thermal-phase change materials (PVT-PCM) system: Energy, exergy and economic analysis, *Renew. Energy*, vol. 136, no. C, pp. 1320–1336, 2019.
- [10] **K. Kant, A. Shukla, A. Sharma, and P. H. Biwole**, Heat transfer studies of photovoltaic panel coupled with phase change material, *Sol. Energy*, vol. 140, pp. 151–161, Dec. 2016, doi: 10.1016/j.solener.2016.11.006.

- [11] **V. Ranawade and K. S. Nalwa**, Multilayered PCMs-based cooling solution for photovoltaic modules: Modelling and experimental study, *Renew. Energy*, vol. 216, p. 119136, Nov. 2023, doi: 10.1016/j.renene.2023.119136.
- [12] **S. Nižetić, M. Jurčević, D. Čoko, and M. Arıcı**, A novel and effective passive cooling strategy for photovoltaic panel, *Renew. Sustain. Energy Rev.*, vol. 145, p. 111164, July 2021, doi: 10.1016/j.rser.2021.111164.
- [13] **A. Al Miaari and H. M. Ali**, Technical method in passive cooling for photovoltaic panels using phase change material, *Case Stud. Therm. Eng.*, vol. 49, p. 103283, Sept. 2023, doi: 10.1016/j.csite.2023.103283.
- [14] **A. Kazemian, M. Hosseinzadeh, M. Sardarabadi, and M. Passandideh-Fard**, Experimental study of using both ethylene glycol and phase change material as coolant in photovoltaic thermal systems (PVT) from energy, exergy and entropy generation viewpoints, *Energy*, vol. 162, pp. 210–223, Nov. 2018, doi: 10.1016/j.energy.2018.07.069.
- [15] **R. Jilte, A. Afzal, and S. Panchal**, A novel battery thermal management system using nano-enhanced phase change materials, *Energy*, vol. 219, p. 119564, Mar. 2021, doi: 10.1016/j.energy.2020.119564.
- [16] **M. Aqib, A. Hussain, H. M. Ali, A. Naseer, and F. Jamil**, Studii de caz experimentale privind efectul nanoparticulelor de Al_2O_3 și nanoparticulelor de carbon din oțel inoxidabil (MWCNT) asupra încălzirii și răcirii PCM, *Case Stud. Therm. Eng.*, vol. 22, p. 100753, Dec. 2020, doi: 10.1016/j.csite.2020.100753.
- [17] **P. B, V. A. A, S. Nižetić, and M. Arıcı**, An experimental investigation on thermal energy storage characteristics of nanocomposite particles dispersed phase change material for solar photovoltaic module cooling, *J. Energy Storage*, vol. 73, p. 109221, Dec. 2023, doi: 10.1016/j.est.2023.109221.
- [18] **G. Wang, B. Wang, X. Yuan, J. Lin, and Z. Chen**, Novel design and analysis of a solar PVT system using LFR concentrator and nano-fluids optical filter, *Case Stud. Therm. Eng.*, vol. 27, p. 101328, Oct. 2021, doi: 10.1016/j.csite.2021.101328.
- [19] **G. Wang, Y. Yao, J. Lin, Z. Chen, and P. Hu**, Design and thermodynamic analysis of a novel solar CPV and thermal combined system utilizing spectral beam splitter, *Renew. Energy*, vol. 155, pp. 1091–1102, Aug. 2020, doi: 10.1016/j.renene.2020.04.024.
- [20] **G. Wang, Z. Zhang, and Z. Chen**, Design and performance evaluation of a novel CPV-T system using nano-fluid spectrum filter and with high solar concentrating uniformity, *Energy*, vol. 267, p. 126616, Mar. 2023, doi: 10.1016/j.energy.2023.126616.
- [21] **H. Liang et al.**, Experimental investigation on spectral splitting of photovoltaic/thermal hybrid system with two-axis sun tracking based on SiO_2/TiO_2 interference thin film, *Energy Convers. Manag.*, vol. 188, pp. 230–240, May 2019, doi: 10.1016/j.enconman.2019.03.060.
- [22] **C. Kandilli**, Performance analysis of a novel concentrating photovoltaic combined system, *Energy Convers. Manag.*, vol. 67, pp. 186–196, Mar. 2013, doi: 10.1016/j.enconman.2012.11.020.
- [23] **G. Wang, F. Wang, F. Shen, Z. Chen, and P. Hu**, Novel design and thermodynamic analysis of a solar concentration PV and thermal combined system based on compact linear Fresnel reflector, *Energy*, vol. 180, pp. 133–148, Aug. 2019, doi: 10.1016/j.energy.2019.05.082.
- [24] **H. Zhang and J. Zhuang**, Research, development and industrial application of heat pipe technology in China, *Appl. Therm. Eng.*, vol. 23, no. 9, pp. 1067–1083, June 2003, doi: 10.1016/S1359-4311(03)00037-1.

- [25] **H. Jouhara, A. Chauhan, T. Nannou, S. Almahmoud, B. Delpech, and L. C. Wrobel**, Heat pipe based systems - Advances and applications, *Energy*, vol. 128, pp. 729–754, June 2017, doi: 10.1016/j.energy.2017.04.028.
- [26] **M. Hu, R. Zheng, G. Pei, Y. Wang, J. Li, and J. Ji**, Experimental study of the effect of inclination angle on the thermal performance of heat pipe photovoltaic/thermal (PV/T) systems with wickless heat pipe and wire-meshed heat pipe, *Appl. Therm. Eng.*, vol. 106, pp. 651–660, Aug. 2016, doi: 10.1016/j.applthermaleng.2016.06.003.
- [27] **E. Johnston, P. S. B. Szabo, and N. S. Bennett**, Cooling silicon photovoltaic cells using finned heat sinks and the effect of inclination angle, *Therm. Sci. Eng. Prog.*, vol. 23, p. 100902, June 2021, doi: 10.1016/j.tsep.2021.100902.
- [28] **K. Mankani, H. Nasarullah Chaudhry, and J. Kaiser Calautit**, Optimization of an air-cooled heat sink for cooling of a solar photovoltaic panel: A computational study, *Energy Build.*, vol. 270, p. 112274, Sept. 2022, doi: 10.1016/j.enbuild.2022.112274.
- [29] **F. Bayrak, H. F. Oztop, and F. Selimefendigil**, Effects of different fin parameters on temperature and efficiency for cooling of photovoltaic panels under natural convection, *Sol. Energy*, vol. 188, pp. 484–494, Aug. 2019, doi: 10.1016/j.solener.2019.06.036.
- [30] **F. Selimefendigil, F. Bayrak, and H. F. Oztop**, Experimental analysis and dynamic modeling of a photovoltaic module with porous fins, *Renew. Energy*, vol. 125, pp. 193–205, Sept. 2018, doi: 10.1016/j.renene.2018.02.002.
- [31] **M. Kong, H. Joo, and H. Kwak**, Experimental identification of effects of using dual airflow path on the performance of roof-type BAPV system, *Energy Build.*, vol. 226, p. 110403, Nov. 2020, doi: 10.1016/j.enbuild.2020.110403.